Magazine of Civil Engineering

ISSN 2712-8172

journal homepage: http://engstroy.spbstu.ru/

Research article

UDC 697.921: 533.697

DOI: 10.34910/MCE.123.7

Vortex zones in an exhaust hood in front of an impermeable plane

A.M. Ziganshin[1] ✉ , ***K.I. Logachev***[2] , ***J.R. Kareeva***[1]

[1] *Kazan State University of Architecture and Engineering, Kazan, Russian Federation*

[2] *V.G. Shukhov Belgorod State Technological University, Belgorod, Russian Federation*

✉ *ziganshin.arslan@gmail.com*

Keywords: local exhaust ventilation, exhaust hood, vortex zone, numerical calculation, impermeable plane

Abstract. The paper presents the results of the study of the flow to the ventilation exhaust device in a form of a circular exhaust hood with a flange, located in front of an impermeable plane. Local exhaust devices are the most rational type of localization of harmful substances in industrial and civil buildings. However, they consume a large amount of energy, so the ways to increase their efficiency are relevant and are the subject of numerous studies around the world. One of the promising ways to reduce the aerodynamic drag of such devices is shaping their inlet sharp edges by the outlines of vortex zones. However, when the hood is located above an impermeable plane, the outlines are not known. This study is carried out numerically, so at the first stage the adequacy of the computation model is demonstrated by comparing it with the known data on the resistance of this kind of devices. Furthermore, the dependences for the local drag coefficient are constructed for the flange dimensions in the range d/R = 0.5; 1.5; 2.5; 5 and distances to the impermeable plane in the range s/R = 0.5; 1; 2; 5. The authors found the outlines of both the first vortex zone, formed at flow separating from the sharp edge of the flange, and the second vortex zone, formed at the point of the flange connection to the exhaust channel. The plotted curves showed that the zones sizes are significantly dependent on the distance s/R. The property of geometric similarity for the first vortex zone was found, which will make it possible to construct the first vortex zone using the dependence for the scale factor without numerical simulation. The constructed outlines of the vortex zones will be further used to develop shaped designs of ventilation exhaust hoods.

Funding: grant of Russian Federation President, Project No.NS-25.2022.4.

Citation: Ziganshin, A.M., Logachev, K.I., Kareeva, J.R. Vortex zones in an exhaust hood in front of an impermeable plane. Magazine of Civil Engineering. 2023. 123(7). Article no. 12307. DOI: 10.34910/MCE.123.7

1. Introduction

The use of local exhaust ventilation significantly increases the efficiency of removal of pollutants emitted in various processes. However, their operation requires a large amount of energy, which is primarily spent to air moving. Depending on the construction of the exhaust system, the required degree of exhaust is provided by a different amount of air. The open local exhaust systems such as exhaust inlets, hoods are characterized by large amounts of air and therefore a very significant energy consumption to overcome the resistance in the network. The efficiency of such systems depends significantly on the distance to the source of effluents: the higher efficiency at a lower flow rate of air removed is achieved for the smaller distance. Usually, the source of effluents is located on the surrounding impermeable plane and it significantly affects the flow to the exhaust. The source of effluents can be a heated part located on a machine tool or conveyor [1], foundry processes [2, 3], joints in welding process [4] or painting process during spray painting of parts extended in space [5, 6], etc. The intrinsic momentum of such pollutants

significantly affects the velocity field of the exhaust device, but it is also important to know the velocity field of exhaust. However, the emitted pollutants can be often considered passive and having no significant influence on the exhaust velocity field. For example, these are diffusive sources of solvent vapor emitted from the painted surface during manual painting and drying [7], vapors of various liquids during drying of construction, plant and other materials [8], fine-dispersed dust emissions [9], aerosols [10]. In this case, the flow in the supply-exhaust system is almost completely determined by the exhaust operation. And it is clear that the presence of an impermeable wall will affect both the velocity field and the outlines of vortex zones (VZs) formed by flow separation at the inlet of such an exhaust. The previous studies on the flow to the circular exhaust showed that two VZs are formed here - the first one when the flow is separated from the sharp edge of the hood, and the second at the point of the hood connection to the channel; moreover, found were the laws for the outlines of the vortex zones and velocity field [11]. It was also shown that the most effective is the design with the hood inclination angle of 90°, i.e. for an exhaust with a flange. So the object of research is the outlines of vortex zones in the circular flanged exhaust hood under the influence of the impermeable plane placed in front of it.

To increase the efficiency and reduce the energy consumption of local exhaust devices, one can use various ways of hiding the source of harmful emission and limiting the area of air flow to the exhaust: curtains [12], flanges at the exhaust and their improvement, for example, by increasing the shielding ability of the flange by placing a supply channel inside it through which the supply stream flows out. Such a design is often called the Aaberg exhaust and is still actively studied [13] and improved in different ways, e.g. by swirling the inflow jet [14]. Methods for capturing emitted pollutants are also being improved, for example by using sound waves to aggregate aerosol particles and increase the efficiency of local exhausts [15]. For example, the numerical assessment of velocity field was carried out for several exhaust hood designs [16], and the corrected formula of axial air flow rate was found. The authors believe that this result also improves the efficiency of local exhaust ventilation, since it clarifies the necessary flow rate removed from the exhaust, although it is clear that during the air removal, there is no actual jet flow, and therefore the axis, so it is important to know not only the velocity at the geometric axis, but also the entire field of velocities in front of the exhaust. Therefore, the velocity and its components in the entire field in front of the exhaust are important when considering the pollutants' removal by exhaust. Nevertheless, in this paper one can also see the formation of vortex zones at the exhaust inlet, although the authors do not pay due attention to it.

Now the reduction of aerodynamic resistance of elements is considered as an efficient approach to improve the efficiency of ventilation systems. A well-known method of reducing resistance of various duct fitting elements consists in installing baffles and blades, which reduce pressure gradients and thus occurring energy losses for flows collisions and creation of separation zones. But these studies are still actual, and such devices are being developed and optimized for different types of ventilation elements – bends [17, 18], tees [19–21], the optimal angle of screen slope in them is being studied [22]. The results obtained show the possibility of reducing the aerodynamic resistance, the level of which depends on the type and size of the duct fitting element, as well as on the flow rate and the ratio of air flow rates for elements with separation or merging of flows. The disadvantage of this method is the complication of the element construction and, the corresponding increase in its cost. Therefore, its application is usually limited by economic considerations. Another way to reduce pressure losses in the elements is smoothing of sharp edges at bends, taps and other junctions, where the flow has a strong deformation and therefore the greatest energy losses. The most common and well-studied method of smoothing is to replace the sharp corner with part of a circle, and the larger circle radius results in a greater resistance reduction. Modern studies continue to optimize the shape of the smoothing curve.

There are examples of finding the optimal spline shape for S-shaped duct section [23], topological optimization of the shape of bends, tees [24, 25] or the so-called biomimetic optimization, when the outlines taken from nature are used for smoothing – the flow of rivers or the growth of plant stems for tees [26, 27], tongue-shaped elbows [25]. These methods also show the possibility of reducing aerodynamic drag, the different level of which depends on the specific design of the element and its parameters. However, this method is not often used in real conditions, where the space placement of ventilation networks is usually limited, because the size of the part improved in this way is more than that of the standard unsmoothed one. The method of installing a shaping insert inside the element does not have the mentioned disadvantage, but the element construction becomes more complicated. For example, inserts of different shapes in unit consisting of an elbow and a tee are investigated in [28], and it is shown that a decrease in resistance is obtained for several cases of the ratio of flow rates through the unit. For the insert, several known profiles from automobile and aircraft construction are chosen.

A specific combination of the described two methods can be considered as profiling the element wall according to the outlines of the vortex zone that occurs when the flow separates from the sharp edge. This does not increase the size and does not complicate the construction of the element, since no additional parts are introduced. But this method has a deeper meaning – the outline for the shape is not chosen conventionally (a circle, ellipse or Bézier curve), but it is the outline of the vortex zone. In other words, the

shaped wall replaces the vortex zone formed in this place of the duct fitting element. Therefore, the profile does not cause the additional narrowing of the channel and deformation of the flow, but only prevents the formation of the flow separation and the associated energy losses.

The outlines of the vortex zones were used to improve the designs of free circular exhaust hoods [29]. This improvement has shown the possibility of reducing the aerodynamic drag by up to 40 % as compared to the original non-shaped ones. Which indicates a significant, but not dominant, contribution of shaping to resistance. The work [29] shows a reduction in the resistance of the inlet sections of freely located exhaust flanged hoods by almost 98 %, by eliminating the second reason – the blockage of the flow resulting from the vortex zone. That is, it is possible to estimate the contribution of the first shaping method to the section resistance at the level of 40 %, and the second – about 58 %. However, the use of the second method increases the dimensions of the system. In practice, in cramped conditions for the placement of elements of ventilation systems, this method is rarely used.

The problem of flow to the flanged exhaust hood in front of impermeable plane was previously solved by the method of discrete vortices [30], and the outlines of the first and second vortex zones (VZs) were found. But due to peculiarities of the mathematical apparatus, the outlines of the second VZ are defined only up to the point of maximum VZ width, and further it extends parallel to the channel wall. However, from general considerations, it is usually assumed that the flow behind the separation zone should occupy the whole channel cross section, so there is a point of closure of the vortex zone to the wall or, in a more general, three-dimensional case – points where the jets of the main flow, surrounding the vortex zone, touch the wall. To develop the improved designs of local exhaust hoods, it is necessary to determine the outlines of VZs along its entire length. This can be done using the methods of computational fluid dynamics, which have shown a fairly good convergence with both the method of discrete vortex in determining the outlines of VZs, and with experimental data on the outlines of VZs and the local drag coefficients (LDC). Such studies for an exhaust hood located freely in space are also presented in [11, 29].

So since the flanged exhaust hood is frequently used for pollutants removal from the impermeable planes and that plane influenced on the flow and the vortex zones, which can be used to shaping and reduce its aerodynamic resistance. It is relevant to find regularities for the full length outlines of the vortex zones for this case.

Therefore, the purpose of the presented paper is to determine the outlines of both the first and the second VZs along their entire length, for the construction of an exhaust hood with an inclination angle of 90°. The objectives to be achieved is to validate the obtained solution and construct the dependences of LDC on the exhaust pipe design and compare with the known data from the reference book [31]; to plot the relationship between the outlines of VZs and both the length of the flange of the exhaust hood, and the distance to the impermeable wall.

2. Methods

The ANSYS Fluent software package is used in this study [32]. The problem is solved in the axisymmetric turbulent formulation. The geometry of the computational domain and its main dimensions are shown in Fig. 1 (for the variant of the problem with dimensions s/R = 2, d/R = 1.5).

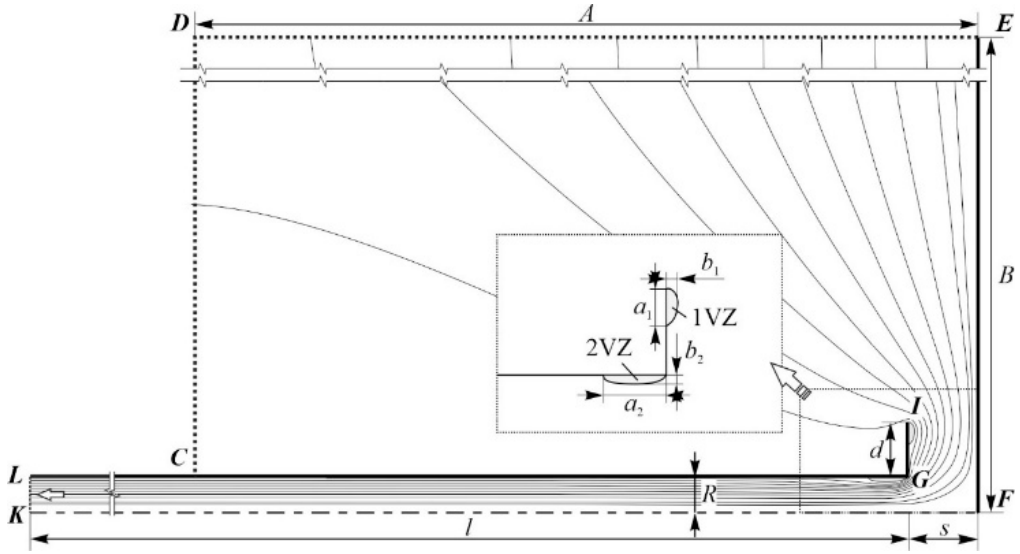

Figure 1. Geometry of the computational domain, streamlines, main dimensions for the variant s/R = 2, d/R = 1.5.

The problem is solved for the hood dimensions d/R = 0.5; 1.5; 2.5; 5 and distances to the impermeable plane s/R = 0.5; 1; 2; 5, where R = 50 mm is the channel radius. For the illustration purposes Fig. 1 also shows the streamlines of the resulting flow. It can be seen that two vortex zones are formed. The first vortex zone (1VZ) is formed at flow separation from the sharp edge of the hood and the second one (2VZ) is formed at flow separation in the point of the hood connection to the exhaust channel. The lengths of vortex zones are a_1 and a_2, respectively, and their widths are b_1 and b_2. Boundary conditions (BC) (Fig. 1) are as follows: a section of external boundary CDE is the free boundary modeled using the "Pressure Inlet" BC with overpressure equal to zero; EF, LGI are impermeable walls (BC "Wall"); KF is the symmetry axis (BC "Axis"); LK is the boundary through which air is removed (BC "Velocity Inlet") with the velocity v_{x0} = 50 m/s. This velocity is assumed to achieve self-similarity and developed turbulent flow regime (Re = $2.9 \cdot 10^5$).

Earlier in [30], a validation for the CFD numerical model has already been performed for the exhaust hood with a flange inclination angle of 0°, i.e. for a circular exhaust opening, and the most adequate combination of the Reynolds Stress Turbulence Model (RSM) with the Enhanced Wall Treatments (EWT) was shown. Therefore, the same combination is used here.

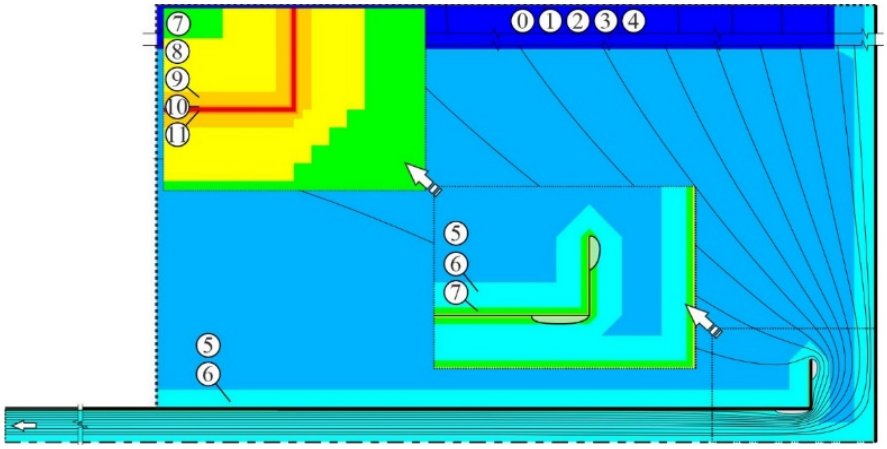

Figure 2. Visualization of adaptation steps for the variant s/R = 2, d/R = 1.5.

To test for grid convergence, each problem underwent a series of computational grid refinement (adaptation) steps when solved (showing with color regions on Fig. 2). The first 4 stages were carried out over the entire computational domain, further the area of refinement was reduced and included part of the area in front of the hood, near the impermeable wall and the channel (No.5). And further, for proper resolution of the boundary layer by the computational grid, refinement was carried out at the solid boundaries – the impermeable plane and the channel walls (adaptations 6 to 11).

Following the results of numerical solution of each refinement stage for each of the investigated geometries, LDC was calculated using the method described in detail in [33]. As a result of numerically obtained distribution of total pressure along the length of the channel, the average value of specific pressure friction loss R (Pa/m) is determined and the zone of non-physical deformation of the pressure field is excluded due to the impact of the boundary condition to determine the channel length l_C (m). Then the LDC value is defined as:

$$\zeta = \frac{P_1^{\text{tot}} - P_2^{\text{tot}} - \Delta P_{\text{fr}}}{P^{\text{dyn}}}, \tag{1}$$

where P_1^{tot} and P_2^{tot} are the total pressure in the section in front of the hood is taken equal to zero, and in the channel section near the outlet boundary, but unaffected by the deformation due to the imposed boundary condition, respectively, $\Delta P_{fr} = R \cdot l_{\text{c}}$ is the pressure loss for friction, $P^{\text{dyn}} = \rho \cdot v_{\text{x0}}^2 / 2$ is the dynamic pressure.

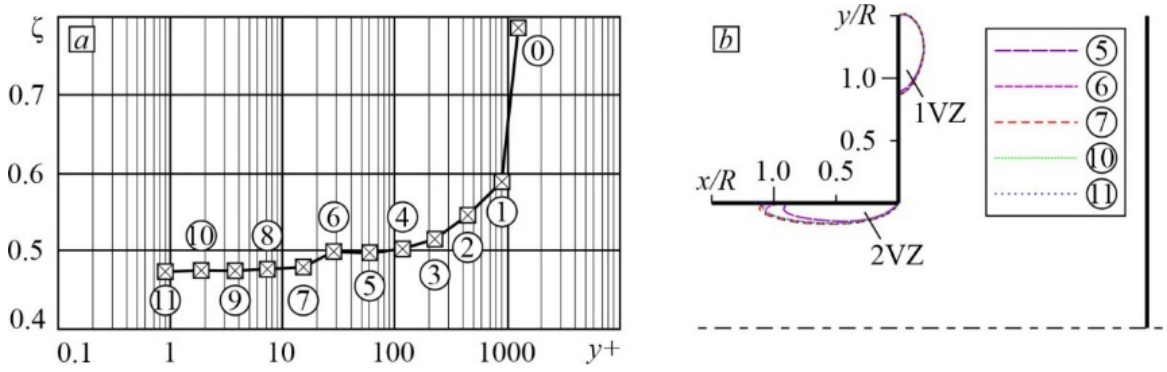

Figure 3. Grid dependence study: a) local drag coefficient; b) vortex zones outlines.

Figure 3a shows the change in LDC during computational grid refinement, which is characterized by dimensionless distance (taking maximum value at all impermeable boundaries at the computational domain) $y+ = \rho \cdot v_\tau \cdot y_p / \mu$, where $v_\tau = \sqrt{\tau_w / \rho}$ is friction velocity, y_p is distance from the center of the near-wall cell to the wall, ρ is density and μ is dynamic viscosity of air at this point, τ_w is shear stress at the wall at this place. It can be seen that with refinement of grid cells and correspondingly decrease of $y+$, LDC changes significantly (5 %–30 %) until $y+$ values are about 30 (adaptation No. 6), then starting from adaptation No.7 ($y+$ <20) the difference between the LDC values does not exceed 0.4 %.

Fig. 3b shows the change in the outlines of the vortex zones (VZ) for several stages of adaptations. The outlines of both the first and second vortex zones for adaptations from No. 7 to No. 11 coincide with each other. This means that there is no grid dependence, so further for all problems a similar refinement process is carried out and the solution on the computational grid No. 11 is taken as the final one. Parameters of computational grids of the last adaptations for different geometries are somewhat different, but are of the same order: sizes of the minimum cell (along solid boundaries) are about 0.01 mm, sizes of the maximum cell (in the underflow area away from exhaust) are about 3 mm, total number of cells is about 2.5 million pcs.

3. Results and Discussion

Numerical solution of all above mentioned designs of the exhaust hood with the flange length d/R = 0.5; 1.5; 2.5; 5 was carried out, for each of them the variants of distances to the impermeable plane s/R = 0.5; 1; 2; 5 were calculated. As a result, the local drag coefficients (LDC) were determined using the calculated pressure field.

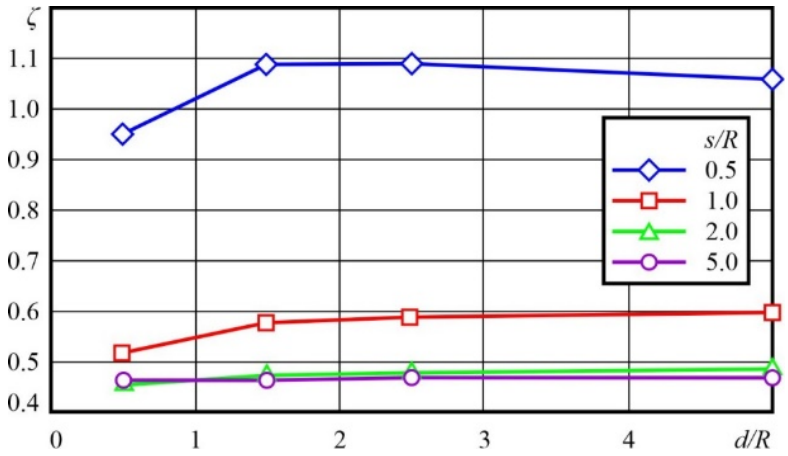

Figure 4. Dependence of local drag coefficient on d/R for various s/R.

When the obtained values are presented as a dependence of ζ on the hood flange length d/R (Fig. 4), one can see that with an increase in d/R, the LDC value increases to $d/R \approx 1.5$. Further, for $d/R > 1.5$, the LDC value stops changing, which indicates the absence of LDC dependence on flange length in the case of long flanges. This is explained by the peculiarities of formation of the first vortex zone, which at such flange lengths closing on it, and further the 2VZ forms separately. It is known that for shorter flanges, the vortex zones merge into one. Nevertheless, for the shortest investigated d/R =1 and d/R =1.5 there seems to be an influence of the first VZ on the second one. In contrast to the case of a free hood [29],

where there is no such dependence for the considered case of a 90° inclination angle. At the same time, there is a significant dependence of LDC on s/R for small distances from the impermeable wall (s/R = 0.5 and s/R = 1). This dependence practically disappears for distances s/R > 2: the curves for s/R = 2 and s/R = 5 practically coincide. This implies that the aerodynamic drag is significantly affected by the impermeable wall at distances less than $2R$.

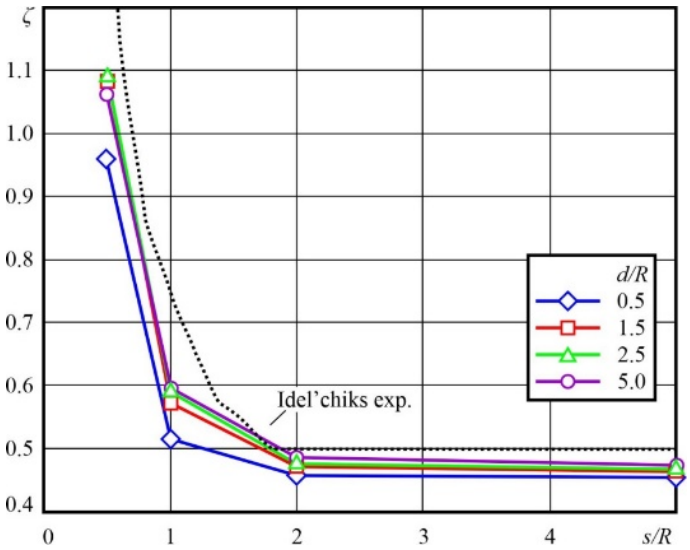

Figure 5. Dependence of local drag coefficient on s/R for various d/R.

To compare the obtained results with the known data [31], we plotted the relationship between LDC and s/R for exhaust designs with different hood flange lengths d/R (Fig. 5). The experimental data [31] (Idel'chiks exp.) are also plotted in Fig. 4. It can be seen that the hood with the smallest flange length (d/R = 0.5) is characterized by somewhat lower resistance than for the other sizes, which is apparently explained by lower constriction and deformation of the flow at small flange lengths. For other flange sizes, the LDC change curve is almost the same. Comparison with the data of [31] shows satisfactory convergence (average difference of about 5 %) of the numerical solution data and the known experimental study. This once again confirms the adequacy of the computation model.

The results of the numerical calculation were used to construct the outlines of the first (1VZ) and second (2VZ) vortex zones for each of the investigated geometries (Fig. 6). The numerically found outlines are shown with solid lines. For comparison, the outlines found by the discrete vortex method (DVM) [30] are also plotted there as dashed lines, and for the exhaust hood with d/R = 5 the outlines for the case of the absence of impermeable wall (s/R = ∞) [29] are shown as dashed line (numerical solution) and dashed-dotted line (DVM).

Although quantitatively the sizes of the first vortex zone found numerically and by DVM are somewhat different, qualitatively the outlines and their size behavior with a change in s/R is similar. For long hoods (d/R ≥ 2.5) the smallest dimensions of VZ (both length and width) are observed at the smallest of investigated distances s/R = 0.5. In this case, the influence of the impermeable wall has a constraining character, limiting the development of the vortex zone. The 1VZ outline in the absence of an impermeable wall, plotted for the case d/R = 5 (dashed line s/R = ∞) shows significantly larger dimensions than those for small s/R. At s/R = 2 the difference between the outlines is 12.2 %, and at s/R = 5 it does not exceed 6.5 %. Thus, the size of 1VZ increases with an increase in distance s/R from 0.5 to 2, and then decreases again for s/R = 5, tending to the size of VZ without an impermeable wall. It can be seen that 1VZ at the smallest distance s/R = 0.5 has a flatter outline, with the smallest width of VZ. 2VZ behaves similarly and at s/R = 5 is no longer significantly different from the case of a free exhaust hood (dashed line s/R = ∞). So, the influence of the wall on VZ disappears at distances of the order of s/R = 5. For a better understanding of the regularities of changes in the dimensions of VZ, the graphs for the length a_1/R and a_2/R and widths b_1/R and b_2/R of the first and second VZ, respectively, are plotted.

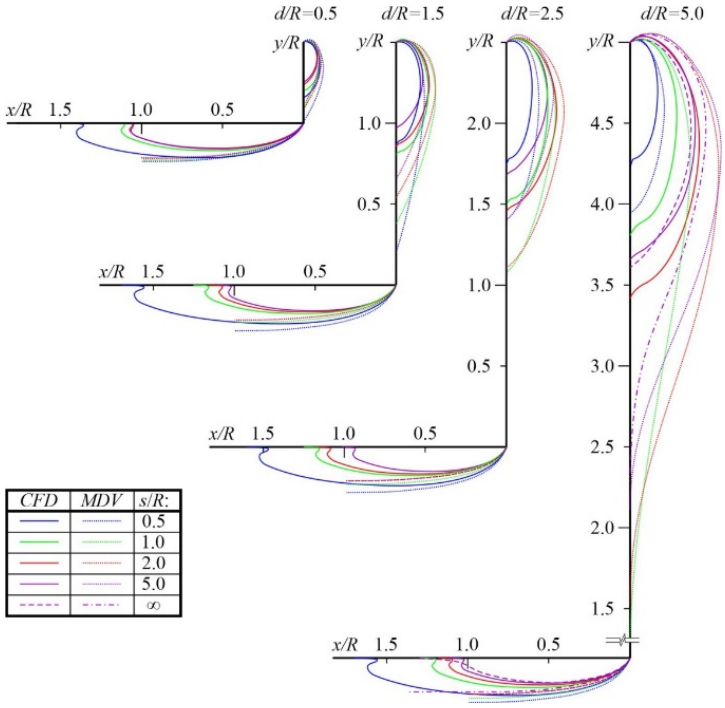

Figure 6. Outlines of vortex zones for various d/R and changing of s/R.

For the main dimensions of VZ (length a and width b) plotted the dependencies for the hood of the studied designs d/R when changing the distance to the impermeable plane s/R. The first VZ is considered in Fig. 7.

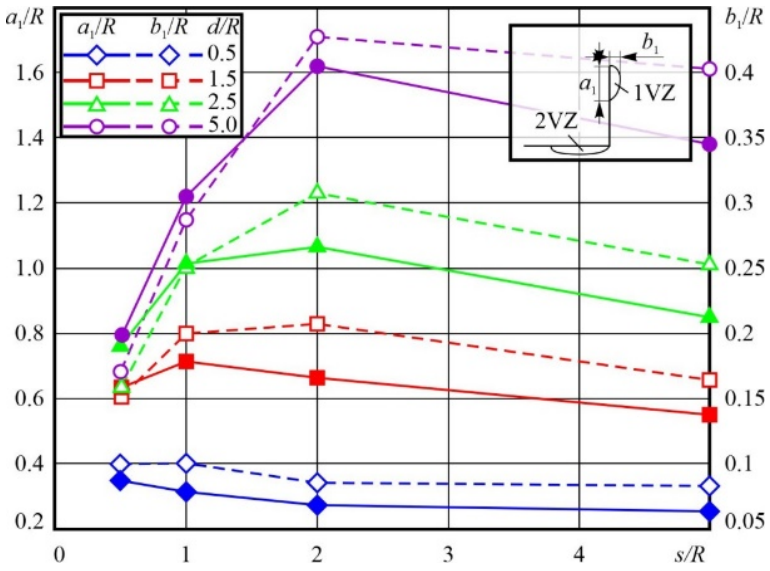

Figure 7. Dependencies of 1VZ dimensions on s/R and d/R.

It can be seen that for each exhaust design (d/R = const), except for the smallest of investigated (d/R = 0.5) with an increase in distance to impermeable surface (s/R) both VZ dimensions increase (mainly up to s/R = 2) and then a smooth decrease is observed. This can be explained by the fact that at small distances, the impermeable plane limits the development of VZ. When the limiting effect decreases, VZ begins to increase, and its size becomes larger than the size of VZ for exhausts without impermeable plane, because the flow velocity when flowing around the sharp edge of the hood flange is significantly higher, due to the presence of impermeable plane. As the distance is further increased, the velocity decreases, resulting in a smooth decrease in the size of VZ to the size of VZ in the absence of an impermeable plane. This states that there are two mechanisms of influence of the impermeable plane on the size of 1VZ – the "damping" mechanism, which leads to a decrease in size, despite the presence of the second mechanism – the mechanism "accelerating" the flow in the area of formation of VZ, which leads to an increase in its size. In general, it can be concluded from Fig. 6 that the "damping" effect of the impermeable plane ends at a distance of about $2R$, and as d/R decreases, this peak shifts toward smaller s/R distances. For the

exhaust hood design with the smallest of the investigated hood flange lengths (d/R = 0.5), the above described dependence can be traced, but has not so pronounced character.

For the second VZ, the patterns of changes in the main dimensions are shown in Fig. 8.

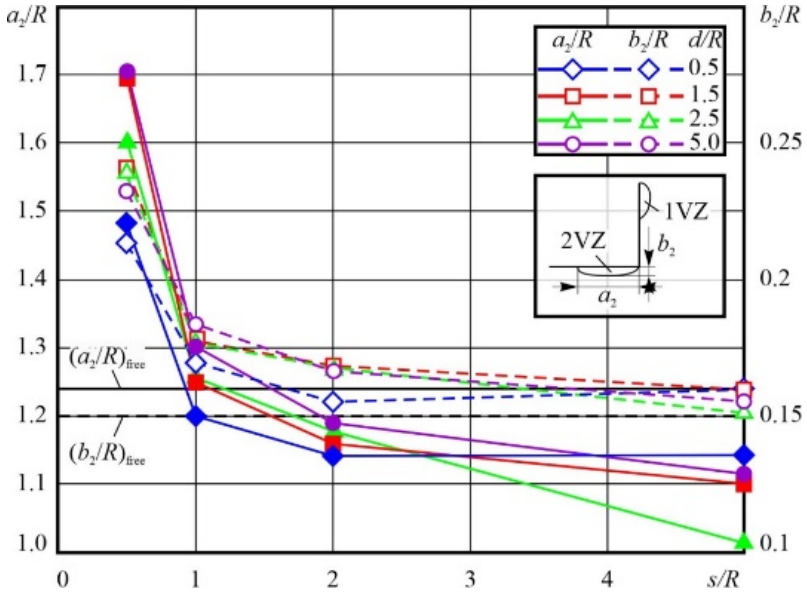

Figure 8. Dependencies of 2VZ dimensions on s/R and d/R.

Both 2VZ sizes decrease as the distance to the impermeable plane increases. This can also be explained by a decrease in the mechanism "accelerating" the flow in the region of 2VZ formation. Decrease of flow velocity, and flow around a sharp inlet edge leads to decrease of sizes of vortex zone. It may be noted that the main decrease in size (by about 20÷40 %) occurs when the distance increases in the range of 0.5 < s/R < 2. Further, the decrease in VZ dimensions is not so significant (about 5 %). Moreover, if 1VZ is characterized by such a change of dimensions, in which they tend to different values for each value of d/R, then for 2VZ for all exhaust hood designs, the dimensions tend to the same value, which is close to the values of dimensions without impermeable plane – $(a_2/R)_{free}$ and $(b_2/R)_{free}$. This is in a good agreement with the earlier studies [11, 22], where it is shown that 1VZ is characterized by a dependence on the size of the exhaust flange, and 2VZ is not characterized.

When analyzing the changes in the 1VZ outlines, their geometric similarity was found, as previously for the case of an exhaust hood located freely [22]. This is expressed in the fact that taking one of the lines of VZ outline as a base line (in this case it is an outline for d/R = 2.5), by multiplying the coordinates of the base line by the scale factor k_{VZ} one can obtain coordinates of 1VZ outlines for other cases (other dimensions of the flange d/R and other distances to the impermeable plane s/R). The dependencies for the scaling factor were constructed using the 1VZ dimensions found from the numerical solution (Table 1).

Table 1. Dependencies for k_{VZ} on d/R and s/R.

s/R	$k_{VZ} = f(d/R)$
0.5	$k_{VZ} = -0.06 \cdot d/R^2 + 0.4548 \cdot d/R + 0.2583$
1	$k_{VZ} = -0.0587 \cdot d/R^2 + 0.5201 \cdot d/R + 0.0603$
2	$k_{VZ} = -0.0334 \cdot d/R^2 + 0.4681 \cdot d/R + 0.0193$
5	$k_{VZ} = -0.0192 \cdot d/R^2 + 0.4026 \cdot d/R + 0.1025$

The behavior of the multipliers in the regression equations can be used to judge that there is a dependence of both k_{VZ} and the 1VZ outlines on the distance to the impermeable plane.

Fig. 9 shows the outlines of 1VZ – the original ones obtained numerically (dashed line), and those found using k_{VZ} (solid line).

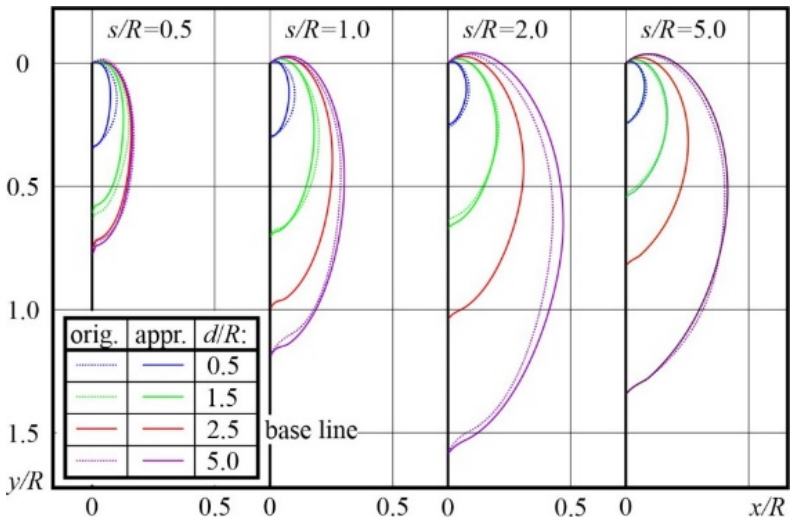

Figure 9. Geometric similarity of the outlines of the first vortex zone.

It can be seen that the 1VZ outlines obtained using the scale factor k_{VZ} (solid lines) coincide well with the original ones found numerically (dashed lines), the difference between them does not exceed 9 %. The exception is the version of the exhaust design with the smallest of the investigated hood flange lengths d/R, at the two smallest of the investigated distances s/R = 1 and 2, where the difference is of the order of 25 %. This indicates some change in the character of the flow in this case, but since for all other designs the use of k_{VZ} shows good results, it can be concluded that in developing improved designs of this type of exhaust, it is necessary to check the efficiency of profiling also for small flange lengths. For the 2VZ outlines, as in the case of free exhausts, no geometric similarity is observed. At the same time, as shown earlier, the 2VZ dimensions for distance s/R > 1 are weakly dependent on design and distance. Therefore, when developing shaped hoods, it will be necessary to check the necessity of using the found outlines for each case, as well as one universal profile, to which, as these studies have shown, the 2VZ outlines tend - the case of a free exhaust hood.

4. Conclusions

The conducted numerical studies of the flow to the ventilating exhaust with an inclination angle of 90°, made it possible to make the following conclusions:

1. To obtain adequate results, both in resistance and in VZ outlines, it is necessary to carry out refinement of computational grid cells in the flow area up to values of parameter $y+$≈60, and further to refine along all solid boundaries up to values of parameter $y+$≈1.

2. The dependence of the local drag coefficient (LDC) is obtained not only on the distance s/R, but also on various flange sizes d/R.

3. VZ outlines for exhaust hood designs with the flange length d/R = 0.5; 1.5; 2.5; 5 and for distances to the impermeable plane s/R = 0.5; 1; 2; 5 have been constructed. Their comparison with those found by the method of discrete vortices has shown satisfactory convergence. So, the detailed outlines for 2VZ were obtained.

4. The dependences of the main dimensions of VZ were plotted. The dimensions of 1VZ increase significantly with an increase in flange d/R, and increase with an increase in distance up to s/R = 2, and then decrease and tend to the dimensions of 1VZ for a free exhaust. The dimensions of 2VZ depend slightly on d/R, and decrease sharply with increasing distance s/R = 2, further changes being insignificant.

5. Geometric similarity for 1VZ is found, and dependencies for the scale factor are constructed to find the outlines of 1VZ, in the size ranges investigated, without involving numerical simulation. There is no geometric similarity for 2VZ.

The obtained results show a significant dependence of both the resistance and the outlines of VZ on the presence of an impermeable plane. So, it should be definitely taken into account for distances $s/R \le 2$. The found outlines of VZ will make it possible to develop improved designs of exhaust hoods with inclination angle of 90°, located in front of the impermeable plane, shaped by the outlines of VZ.

References

1. Kulmala, I., Hynynen, P., Welling, I., Säämänen, A. Local ventilation solution for large, warm emission sources. The Annals of occupational hygiene. 2007. 51(1). Pp. 35–43. DOI: 10.1093/annhyg/mel049
2. Huang, Y., Wang, Y., Liu, L., Nielsen, P. V., Jensen, R.L., Yang, X. Performance of constant exhaust ventilation for removal of transient high-temperature contaminated airflows and ventilation-performance comparison between two local exhaust hoods. Energy and Buildings. 2017. 154. Pp. 207–216. DOI: 10.1016/j.enbuild.2017.08.061
3. Huang, Y., Wang, Y., Liu, L., Nielsen, P.V., Jensen, R.L., Yan, F. Reduced-scale experimental investigation on ventilation performance of a local exhaust hood in an industrial plant. Building and Environment. 2015. 85. Pp. 94–103. DOI: 10.1016/j.buildenv.2014.11.038
4. Flynn, M.R., Susi, P. Local exhaust ventilation for the control of welding fumes in the construction industry--a literature review. The Annals of occupational hygiene. 2012. 56 (7). Pp. 764–76. DOI: 10.1093/annhyg/mes018
5. Madsena, U., Fontaine, J.R., Nielsenc, P. V., Aubertin, G., Breum, N.O. A Numerical Study of Dispersion and Local Exhaust Capture of Aerosols Generated from a Variety of Sources and Airflow Conditions. AIHAJ. 1996. 57 (2). Pp. 134–141. DOI: 10.1202/0002-8894(1996)057<0134:ANSODA>2.0.CO;2
6. Liu, F., Zhang, T.T., Zhang, H., Huo, Q., Wang, J., Long, Z., Liu, J. Removing painting-generated VOCs in a commercial airplane hangar with multiple portable exhaust hoods. Building and Environment. 2021. 196 (January). Pp. 107797. DOI: 10.1016/j.buildenv.2021.107797
7. Qi, Y., Shen, L., Zhang, J., Yao, J., Lu, R., Miyakoshi, T. Species and release characteristics of VOCs in furniture coating process. Environmental Pollution. 2019. 245. Pp. 810–819. DOI: 10.1016/j.envpol.2018.11.057
8. Cao, W.-x., You, X.-y. The inverse optimization of exhaust hood by using intelligent algorithms and CFD simulation. Powder Technology. 2017. 315. Pp. 282–289. DOI: 10.1016/j.powtec.2017.04.019
9. Zamalieva, A.T., Ziganshin, M.G., Potapova, L.I. Ob jeffektivnosti sushhestvujushhih metodov ciklonnoj fil'tracii pri osazhdenii melkodispersnyh chastic klassov PM10, PM2,5 [The analysis of efficiency of use of a cyclonic filtration for sedimentation of fine particles]. News of KSUAE. 2017. 42 (4). Pp. 415–423.
10. Bilalov, M.I., Ziganshin, M.G. Estimates of the influence of the solar irradiation spectrum energy on the intensity of heat treatment of solid waste with hexavalent chromium. IOP Conference Series: Materials Science and Engineering. 2019. 481. Pp. 012044. DOI: 10.1088/1757-899X/481/1/012044
11. Logachev, K.I., Ziganshin, A.M., Averkova, O.A., Logachev, A.K. A survey of separated airflow patterns at inlet of circular exhaust hoods. Energy and Buildings. 2018. 173 (6). Pp. 58–70. DOI: 10.1016/j.enbuild.2018.05.036
12. Wang, J., Huo, Q., Zhang, T., Liu, F., Wang, S., Ma, Z., Jiang, S. Performance evaluation for a coupled push – pull ventilation and air curtain system to restrict pollutant dispersion in a factory building. Journal of Building Engineering. 2021. 43 (January). Article no. 103164. DOI: 10.1016/j.jobe.2021.103164
13. Zhang, J., Wang, J., Gao, J., Cao, C., Lv, L., Xie, M., Zeng, L. Critical velocity of active air jet required to enhance free opening rectangular exhaust hood. Energy and Buildings. 2020. 225. Article no. 110316. DOI: 10.1016/j.enbuild.2020.110316
14. Zhao, R., Qian, H., Liu, L., Zheng, X. Comprehensive performance evaluation of a novel Aaberg exhaust system reinforced by a swirling jet. Building and Environment. 2020. 167. Article no. 106451. DOI: 10.1016/j.buildenv.2019.106451
15. Vekteris, V., Tetsman, I., Mokshin, V. Investigation of the efficiency of the lateral exhaust hood enhanced by aeroacoustic air flow. Process Safety and Environmental Protection. 2017. 109. Pp. 224–232. DOI: 10.1016/j.psep.2017.04.004
16. Pinelli, M., Suman, A. A numerical method for the efficient design of free opening hoods in industrial and domestic applications. Energy. 2014. 74. Pp. 484–493. DOI: 10.1016/j.energy.2014.07.014
17. Yin, Y., Li, A., Wen, X., Zhang, J., Zhang, X., Guo, J., Li, J., Zhang, W., Che, J. Resistance reduction of an elbow with a guide vane based on the field synergy principle and viscous dissipation analysis. Journal of Building Engineering. 2022. 54. Article no. 104649. DOI: 10.1016/j.jobe.2022.104649
18. Solodova, E.E. Osobennosti chislennogo modelirovaniya techeniy v Z-obraznykh otvodakh sistem ventilyatsii i konditsionirovaniya zdaniy i sooruzheniy [Features of flows numerical modeling in z-shaped elbows of ventilation and air conditioning systems of buildings and structures. News of KSUAE. 2021. 55 (1). Pp. 71–84. DOI: 10.52409/20731523_2021_1_71
19. Yin, Y., Wen, X., Zhang, J., Li, A. Geometric parameters optimization of low resistance T-junction with guide vanes in HVAC system. E3S Web of Conferences. 2022. 356. Article no. 02056. DOI: 10.1051/e3sconf/202235602056
20. Shopayeva, A., Safiullin, R. CFD-modeling of flow in confluence nodes of ventilation units of multi-storey buildings. IOP Conference Series: Materials Science and Engineering. 2020. 890. Pp. 012157. DOI: 10.1088/1757-899X/890/1/012157
21. Gao, R., Liu, K., Li, A., Fang, Z., Yang, Z., Cong, B. Study of the shape optimization of a tee guide vane in a ventilation and air-conditioning duct. Building and Environment. 2018. 132. Pp. 345–356. DOI: 10.1016/j.buildenv.2018.02.006
22. Yin, Y., Chen, K., Qiao, X., Lin, M., Lin, Z., Wang, Q. Mean Pressure Distributions on the Vanes and Flow Loss in the Branch in a T Pipe Junction with Different Angles. Energy Procedia. 2017. 105. Pp. 3239–3244. DOI: 10.1016/j.egypro.2017.03.718
23. Srinivasan, K., Balamurugan, V., Jayanti, S. Shape optimisation of curved interconnecting ducts. Defence Science Journal. 2015. 65 (4). Pp. 300–306. DOI: 10.14429/dsj.65.8353
24. Courtais, A., Lesage, F., Privat, Y., Frey, P., Latifi, A. razak. Adjoint system method in shape optimization of some typical fluid flow patterns. Computer Aided Chemical Engineering. 2019. 46. Pp. 871–876. DOI: 10.1016/B978-0-12-818634-3.50146-6
25. Demirel, G., Acar, E., Celebioglu, K., Aradag, S. CFD-driven surrogate-based multi-objective shape optimization of an elbow type draft tube. International Journal of Hydrogen Energy. 2017. 42 (28). Pp. 17601–17610. DOI: 10.1016/j.ijhydene.2017.03.082
26. Gao, R., Zhang, H., Li, A., Liu, K., Yu, S., Deng, B., Wen, S., Li, A., Zhang, H., Du, W., Deng, B. A novel low-resistance duct tee emulating a river course. Building and Environment. 2018. 144 (June). Pp. 295–304. DOI: 10.1016/j.buildenv.2018.08.034
27. Gao, R., Liu, K., Li, A., Fang, Z., Yang, Z., Cong, B. Biomimetic duct tee for reducing the local resistance of a ventilation and air-conditioning system. Building and Environment. 2018. 129 (September 2017). Pp. 130–141. DOI: 10.1016/j.buildenv.2017.11.023
28. Li, A., Chen, X., Chen, L. Numerical investigations on effects of seven drag reduction components in elbow and T-junction close-coupled pipes. Building Services Engineering Research and Technology. 2015. 36 (3). Pp. 295–310. DOI: 10.1177/0143624414541453
29. Logachev, K.I., Ziganshin, A.M., Averkova, O.A. On the resistance of a round exhaust hood, shaped by outlines of the vortex zones occurring at its inlet. Building and Environment. 2019. 151. Pp. 338–347. DOI: 10.1016/j.buildenv.2019.01.039

30. Logachev, K.I., Ziganshin, A.M., Huang, Y., Wang, Y., Averkova, O.A., Popov, E.N., Gol'tsov, A.B., Tiron, O. V. Investigating changes in geometric dimensions of vortex zones at the inlet of an exhaust hood set over a plane. Building and Environment. 2022. (May). Pp. 109377. DOI: 10.1016/j.buildenv.2022.109377
31. Idel'chik, I.E., Steinberg, M.O. Handbook of Hydraulic Resistance. 3rd Edn. . Boca Raton, FL, CRC Press, 1994. 790 s. ISBN: 0-8493-9908-4.
32. ANSYS® Academic Research Mechanical and CFD, Release 18.2.
33. Logachev, K.I., Ziganshin, A.M., Averkova, O.A. Simulations of dust dynamics around a cone hood in updraft conditions. Journal of Occupational and Environmental Hygiene. 2018. 15 (10). Pp. 715–731. DOI: 10.1080/15459624.2018.1492137

Information about authors:

Arslan Ziganshin, *Doctor of Technical Sciences*
ORCID: https://orcid.org/0000-0001-7335-7797
E-mail: ziganshin.arslan@gmail.com

Konstantin Logachev, *Doctor of Technical Sciences*
ORCID: https://orcid.org/0000-0003-0632-6784
E-mail: kilogachev@mail.ru

Julia Kareeva, *PhD in Technical Sciences*
ORCID: https://orcid.org/0000-0002-9497-349X
E-mail: jkareeva2503@gmail.com

Received 13.04.2023. Approved after reviewing 25.09.2023. Accepted 27.09.2023.